We are IntechOpen,
the world's leading publisher of
Open Access books
Built by scientists, for scientists

6,100
Open access books available

149,000
International authors and editors

185M
Downloads

154
Countries delivered to

Our authors are among the

TOP 1%
most cited scientists

12.2%
Contributors from top 500 universities

BOOK
CITATION
INDEX
CLARIVATE ANALYTICS
INDEXED

WEB OF SCIENCE™

Selection of our books indexed in the Book Citation Index
in Web of Science™ Core Collection (BKCI)

Interested in publishing with us?
Contact book.department@intechopen.com

Numbers displayed above are based on latest data collected.
For more information visit www.intechopen.com

Chapter

Quantum Dots as Material for Efficient Energy Harvesting

Paweł Kwaśnicki

Abstract

The essence of the photovoltaic effect is the generation of electric current with the help of light. Absorption of a quantum of the energy of light (photon) generates the appearance of an electron in the conduction band and holes in the valence band. The illumination of the material, in general, is not uniform, which leads to the appearance of spatially inhomogeneous charge in the band valence and conductivity. Besides, electrons and holes generally diffuse with different velocities, which leads to the creation of a separated space charge and generation of an electric field (sometimes called the Dember field). This field inhibits further separation of cargo. The reverse processes also take place in the system, i.e. electron recombination and holes. These processes are destructive from the point of view of photovoltaics and should be minimized, which is achieved; thanks to the spatial separation of electrons and holes. The point is that electrons and holes were carried away from the area where they formed as quickly as possible, yes to prevent their spontaneous recombination. The use of semiconductor quantum dots introduced into the photoelectric material is currently a very important and effective way to increase the efficiency of photoelectric devices and photovoltaic cells. This is due to the fact that in semiconductor photoelectric materials with no quantum dots, there is always some upper limit of the wavelength $\lambda_{gr}[gr] \simeq 1,24/E_g[eV]$ for absorbed light, above which the light is not absorbed.

Keywords: quantum dots, photovoltaic, QDSC, transparent PV

1. Introduction

The maximum coefficient of light to electric conversion in semiconductor systems is determined by the so-called Shockley-Queisser limit, which is approximately 32% with the optimal width of the band gap of $1.2-1.3$ eV. However, performance can be improved by using solutions based on semiconductor nanostructures [1–2]. Such cells are called Third Generation Photovoltaic Cells (KFTG). One type of nanostructure that plays an important role is the so-called quantum dots, that is, small semiconductor grains with sizes in the order of nm. As bounded systems in all three dimensions, quantum dots are characterized by a discrete energy spectrum. The advantage of such systems is the fact that due to the lack of translational symmetry, the limitation on quantum transitions resulting from the behaviour of the wave vector (equality of the photon and electron wave vector) is removed. Exclusion of this limitation leads to the

fact that absorption can arise from deep discrete levels to high energy states. As a result, the useful range of the light spectrum expands considerably towards violet light. However, the width of the energy gap of the output semiconductor limits the possibility of using the spectral part from the low-energy light side [3].

Another beneficial element resulting from the location of an electron and a hole (exciton) in the area of a quantum dot is the slowing down of thermalization processes and increasing the effective number of generated carriers through transitions in which the exciton while relaxing to lower energy, generates another exciton (the phenomenon of multiple exciton generation) [1]. Thermalisation occurs when carriers transfer their excess energies to the crystal lattice through interaction with phonons. In this way, large populations of non-equilibrium (hot) charges are created and the carriers lose their energy to the lattice vibrations. Thermalisation times depend on many factors such as carrier concentration and lattice temperature but are usually in the range below 100 ps. The multiple generations of an exciton can only occur for high-energy photons, due to the conservation of energy principle. This effectively means that one photon can generate two (or more) carriers. Of course, there are also recombination processes in which the exciton generated in the photon absorption process disappears. All these factors mean that the performance of such systems may exceed the Shockley-Queisser limit.

Numerous types of quantum dots can be used in photovoltaics: semiconductor polycrystalline and granular materials, quantum dots obtained by epitaxial methods or from colloidal solutions, nanoparticles of organic dyes, etc. There are also many possibilities for the architecture of photovoltaic cells. Their common feature is that the phenomenon of multiple exciton excitation in dots is used, and the generated charges (electrons and holes) are discharged in various ways to the electrodes while ensuring their spatial separation. One possibility is to use dots dispersed in the conductive material (e.g. in organic polymers). With the appropriate concentration of the dots, the discharge of the charge from the dots to the electrodes can take place due to the coupling between the quantum dots. In the case of regular networks of dots (one, two or three-dimensional), discrete dot states are formed into mini-electron bands, ensuring charge transport. This problem has been and is still widely studied in the literature [4, 5].

Photovoltaic cells using regular quantum dot networks and their electronic miniband structure (also called intermediate bands) have become one of the significant directions of photovoltaics development [6]. The essence of this type of solution is the fact that in the area between the electrodes in the p-n junction there is a layer with quantum dots between which the distance is so small that an intermediate band is created in this area. This allows the use of low-energy photons (with energy lower than the width of the output semiconductor gap) to generate electrons in the conduction band and holes in the valence band. This is due to the optical transitions from the valence band to the intermediate band and from the intermediate band to the conduction band. An important element is also the fact that recombination processes are much less likely in the case of the intermediate band than in the case of isolated quantum dots. In this case, it is enough for the wave functions of the dots to be quite delocalized. This can be achieved in systems with complexes of quantum dots instead of regular lattices [7].

2. A single quantum dot

First, consider a single semiconductor quantum dot. In general, the quantization associated with the limited size of the quantum dot leads to discrete energy values, ε_n

(n = 1,2,3 …). Each eigenvalues value corresponds to an orbital wave function ψ_n (**r**). For the sake of simplicity, we ignore the magnetic and spin-orbital interactions in this consideration. Then, we deal with a two-fold spin degeneration of all discrete levels of a quantum dot. However, if there are spin-orbital or other magnetic forces in the system, then this degeneration is generally cancelled out. A diagram of the discrete levels of a semiconductor quantum dot in some other semiconductor matrix is shown in **Figure 1**. The energy gap, both in the matrix and in the material of which the dot is made of, is marked with a dashed line (the bottom of the conductivity band and the upper limit of the valence band).

Both the own energy values and the corresponding wave functions fulfil the Schrodinger equation:

$$\left[-\frac{\hbar^2}{2m} \left(\frac{\partial^2}{\partial x^2} + \frac{\partial^2}{\partial y^2} + \frac{\partial^2}{\partial z^2} \right) + V(\boldsymbol{r}) \right] \psi_n\ (\boldsymbol{r}) \equiv \hat{H}\psi_n(\boldsymbol{r}) = \varepsilon_n \varnothing_n(\boldsymbol{r}) \qquad (1)$$

where V (**r**) is the limiting potential of the quantum dot, and $\hat{H}$ is the operator of the total energy, that is kinetic and potential energy.

2.1 Two interacting quantum dots

Let us now consider two quantum dots at some distance from each other. Let us assume that the separation of levels on the dots is large enough and consider only one discrete level in a selected dot and the closest discrete level in the second dot. Let us assume that the other levels are sufficiently distant on the energetic scale. Let us denote this level in the first dot as ε_1 and in the second dot as ε_2. If the dots were identical, then $\varepsilon_1 = \varepsilon_2$, but in general these energies may be different. We denote the corresponding normalized wave functions as $\psi_1(\boldsymbol{r})$ and $\psi_2(\boldsymbol{r})$. If these dots are close enough and their wave functions partially overlap, then the wave functions of a system composed of two dots can be taken in the form

$$\psi(\boldsymbol{r}) = a\psi_1(\boldsymbol{r}) + b\psi_2(\boldsymbol{r}) \qquad (2)$$
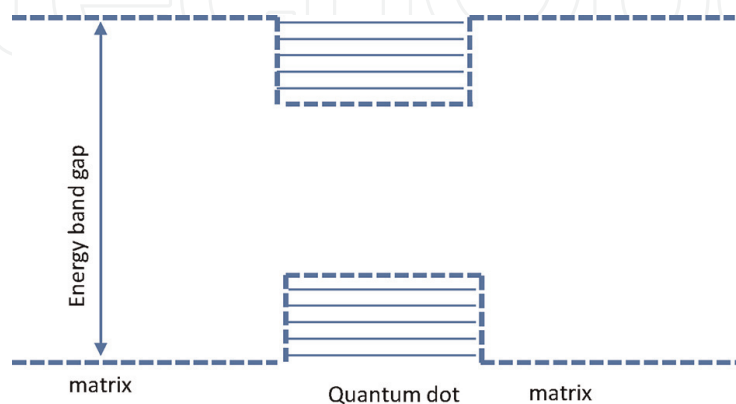

Figure 1.
A diagram of the energy structure of a single semiconductor quantum dot placed in a matrix made of another semiconductor material. The dashed line corresponds to the location of the bottom of the conduction band and the upper limit of the valence band in the semiconductor matrix and in the material of which the semiconductor quantum dot is made. The solid lines represent the discrete energy levels of the quantum dot.

where a and b are constants. When the wave functions are not too large, one can put the normalization condition $|a|^2 + |b|^2 = 1$. The energies of the system, $E = \langle \hat{H} \rangle$, can then be written in the form

$$E = \varepsilon_1 + \varepsilon_2 + a*b \int dr \psi_1^*(r) V_1(r) \psi_2(r) + ab^* \int dr \psi_2^*(r) V_2(r) \psi_1(r) \qquad (3)$$

where $V_1(r)$ and $V_2(r)$ are the limiting potentials for both quantum dots.

If the dots are the same, so they have the same limiting potential, $V_1(\mathbf{r}) = V_2(\mathbf{r-d}) \equiv V(\mathbf{r})$, where d is the vector connecting the dots 1 and 2, and the same levels energy $\varepsilon_1 = \varepsilon_2 \equiv \varepsilon$, and the same corresponding wave functions, $\psi_1(\mathbf{r}) = \psi_2(\mathbf{r-d}) \equiv \psi(\mathbf{r})$, then the energies of the system can be written in the form

$$E = 2\varepsilon + (a*b + ab*) \int dr \psi^*(r) V(r) \psi(r - d) \qquad (4)$$

The state corresponding to a = b ($|a| = |b| \, 1/\sqrt{2}$) is a symmetric state with energy ε_2- t and the antisymmetric state, a = −b, is a state with energy ε_2 + t, where

$$t = - \int dr \psi^*(r) V(r) \psi(r - d) \qquad (5)$$

The hoping parameter t is positive because V (r) as the attracting potential is negative. The symmetric state is the binding (lower energy) state, while the antisymmetric state is the anti-binding (higher energy) state.

2.2 Periodic networks of quantum dots

Now, let us consider the periodic networks of quantum dots and first consider the one-dimensional periodic chain of equal quantum dots. The wave function then satisfies Bloch's theorem, $\psi(\mathbf{r + d}) = \psi(\mathbf{r})$ exp. iQ•d where Q is a wave vector, Q = (Q, 0, 0) and d = (d, 0, 0). Consider a chain with N dots and assume periodic Born-Karman conditions. From the considerations, so far, it follows that the energies of such a chain can be written in the form

$$E = \sum_l \varepsilon_l + \frac{1}{2} \sum_l (a_l a_{l+1} t_{l,l+1} + a_l a_{l-1} t_{l,l-1}) \qquad (6)$$

where a_l is the amplitude of the wave function at node l, l = 1, ... N, and summing over l means summing over all N nodes. Factor 1/2 in the second term eliminates double counting of hoping terms. In turn $t_{l, \, l \pm 1}$ means the element hoping to the nearest neighbours. It follows from Bloch's theorem that $a_{l \pm 1} = a_l$ exp. $\pm$ iQd. Considering the constant value of the hoping term, $t_{l, \, l \pm 1} = t$, and the constant value of the discrete energies, $\varepsilon_l = \varepsilon$, the total energy can be written as

$$E = N\varepsilon + t\cos Qd \qquad (7)$$

The one-dimensional wave vector takes the following values: Q = $(2\pi/d)$ l for l = 0, $\pm 1, \cdot \pm$ N. The electronic states thus form an energy band with a width of 2 t. This can be interpreted in such a way that, in the case of the interacting dots, the discrete levels
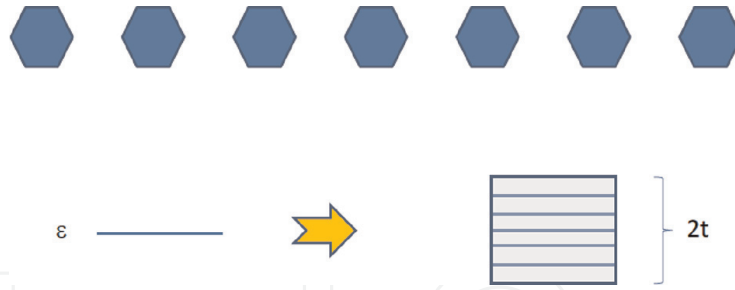
Figure 2.
Diagram of the energy structure of a one-dimensional network of interconnected quantum dots. In the case of a large number of dots in the chain, a continuous energy band with a width of 2 t is created, corresponding to the shaded area.

blur to form an energy band, as shown schematically in **Figure 2**. This figure shows a finite (and relatively small) number of quantum dots, so the energy levels of the entire system are a discrete structure. The original degeneracy is abolished. However, in the case of a long chain, the states resulting from the interaction between the dots create a continuous (at the limit of an infinitely long one-dimensional network) energy band with a width of 2 t. In **Figure 2**, this band is marked with a shaded area in which discrete levels are visible.

In the case of a two-dimensional rectangular quantum dot network, where the interaction between the dots is the same for all four closest neighbours, the bandwidth resulting from the interaction is greater due to the greater number of the nearest neighbours and amounts to 4 t. This is shown schematically in **Figure 3**. Similar to **Figure 2**, the energy structure diagram is shown for a finite number of quantum dots (49 to be exact). The energy band resulting from the discrete levels corresponds to the shaded area. The discrete structure resulting from a finite number of dots is now virtually indistinguishable in this figure. In the case of a network with N × N dots, the band becomes continuous for large values of N (more precisely for N ➔ ∞).

Similarly, the three-dimensional network of quantum dots can be described. As in the above-discussed cases of the one-dimensional and two-dimensional dot network, the interaction between the dots leads to the formation of an energy band from the discrete level of individual dots. However, the width of this band in the three-dimensional case is greater and amounts to 6 t for the cubic quantum dot network.

In summary, discrete levels in periodic quantum dot networks blur to form an energy band. The width of this band depends on the value of the hoping parameter t, and it decreases to zero with $t \rightarrow 0$. Besides, the bandwidth also depends on the number of the nearest neighbours, which is 2 t for a one-dimensional chain, 4 t for a two-dimensional square lattice, and 6 t for a three-dimensional cubic lattice.

An important aspect of the resulting band structure is the fact that the electronic states are stretched as opposed to the localized states of a single dot. Electrons and holes are therefore mobile in these bands and can be led relatively easily to the appropriate electrode, even if their generation takes place at a considerable distance. Moreover, the value of the parameter t depends on the wave function of the given energy level of the quantum dot. Therefore, the widths of the mini-bands resulting from the levels of a quantum dot can vary significantly from level to level.

2.3 Non-periodic systems

Let us now consider non-periodic systems in which quantum dots of various shapes and sizes are arranged randomly. In such systems, the connection between the
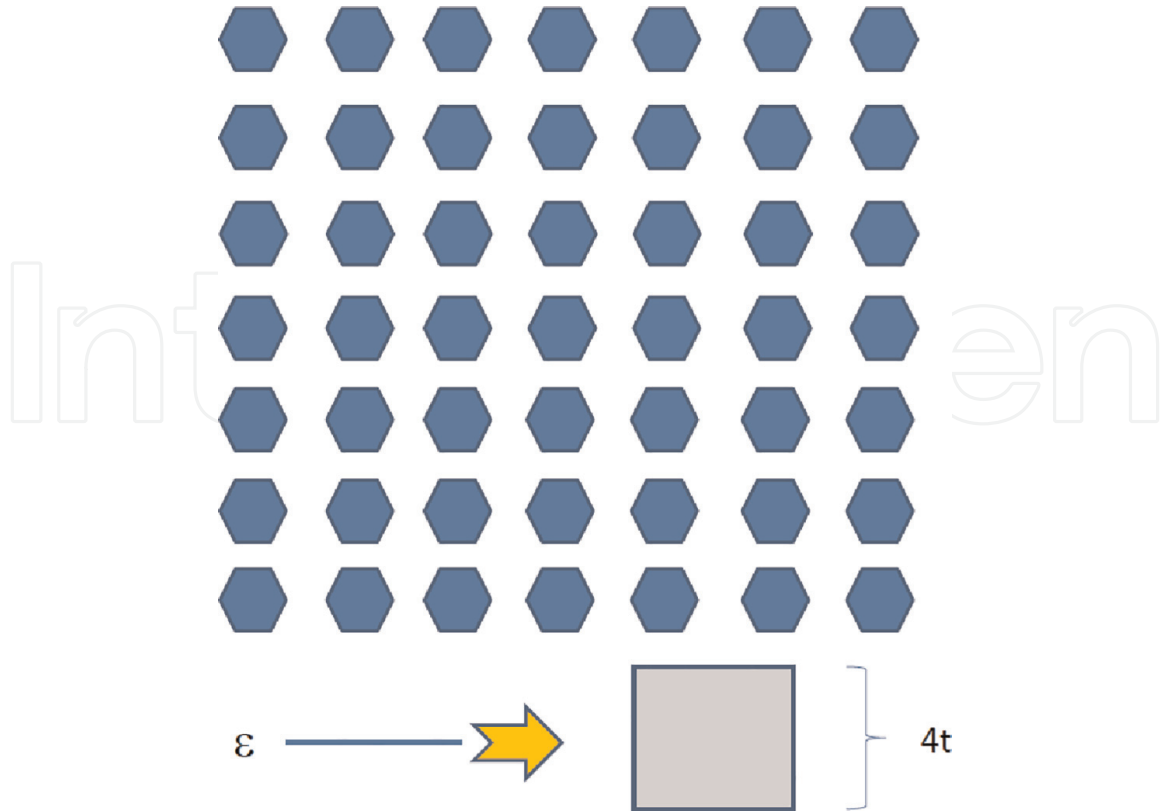
Figure 3.
Diagram of the electronic structure in the case of a two-dimensional network of interconnected quantum dots. In the case of a large (unlimited) two-dimensional network, a continuous 4 t wide energy band is created (discrete structure from a finite number of dots is now virtually indistinguishable).

dots is also described by random hoping parameters. Moreover, if the dots are arranged quite rarely, then only some of them are connected together. In the simplest case, such a system includes complexes of two or three interconnected quantum dots. In the simplest model system, the complexes of double dots are arranged randomly, and it can be assumed that the coupling parameter between two dots and the eigen energies of individual dots in the complex are statistically different. If the energies of states in dot 1 and 2 are ε_1 and ε_2, respectively, and the coupling parameter is t, then the eigen energies of the interacting complex, ε_- for the bonding state and ε_+ for the anti-bonding state, are respectively

$$\varepsilon_{\pm} = \frac{1}{2}(\varepsilon_1 + \varepsilon_2) \pm \frac{1}{2}\sqrt{(\varepsilon_1 - \varepsilon_2)^2 + 4t^2} \qquad (8)$$

The appropriate wave functions are located on the dots and in the space between the dots. If the colon complexes are different, then a spectrum of discrete levels located in different areas of the matrix is effectively obtained.

In the case of triple complexes, in which three dots are connected together to form one complex, the coupling is described by two hoping parameters, and the interaction result produces three different discrete levels located on the complex and in the space between the dots.

In the case of networks with relatively small deviations from the translational symmetry, the interaction between the dots leads to the formation of a continuous band. However, the corresponding wave functions may be localized. The length of the location, that is, figuratively speaking of the number of quantum dots in the area of

which the wave function related to a given electron state extends, may be large enough, comparable to the size of the structure, so effectively such states meet the mobility conditions needed for pairing electrons and holes.

3. Two-dimensional cells with chains of quantum dots

Let us now consider examples of possible planar photovoltaic cells containing one-dimensional networks of quantum cells. The simplest such structure is shown in **Figure 4**. Quantum dots are embedded in a thin layer of optically active semiconductor, which form one-dimensional chains. The distance between the strings is so long that the interaction between dots from different strings can be ignored. This interaction is non-zero only for the adjacent dots in a given string. If the quantum dots within one chain are the same, then the interaction between the dots generates energy bands from discrete levels of quantum dots. The electrons and holes generated in a certain quantum dot can then freely flow to the appropriate electrode (collecting electrons or holes). This is possible because the states in the electron bands made of discrete dot levels are conductive. If both electrodes were the same, then there would be no such separation. Note that the condition is the formation of bands from discrete dot levels, however, these bands may be different within different chains. Thus, a more general version of the photovoltaic cell shown in **Figure 4** would be a cell in which each of the strings would be composed of other quantum dots (however, the same in the given chain).

However, even in this case, the same electrodes can be achieved by means of appropriate modulation of quantum dots. Besides, such a modified arrangement of dots should also strengthen the separation in the case of two different electrodes (as in **Figure 4**). Well, if quantum dots in a given chain will gradually change their sizes (in any direction), as shown schematically in **Figure 5**, then the energies of a given dot level will gradually increase for electrons and decrease for holes (or vice versa). In **Figure 5**, shown quantum dots are stretched in one direction but one can consider different direction. The change of dot parameters is so small that the shift of a given level is much smaller than the distance between the nearest discrete levels. Then the
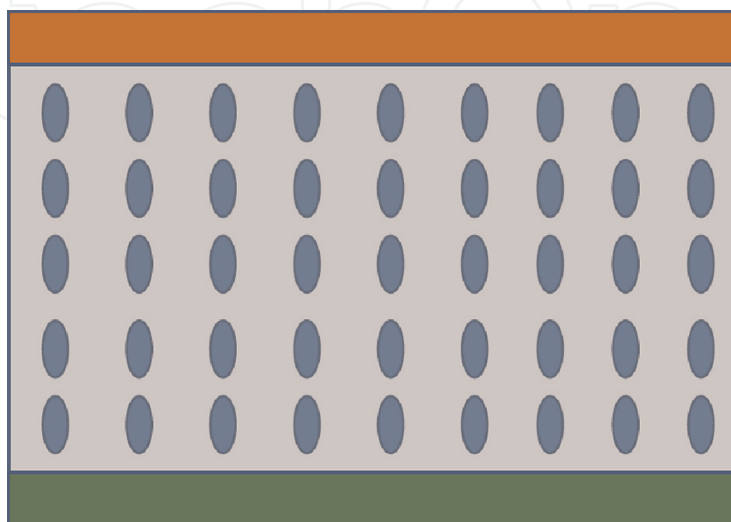
Figure 4.
Diagram of a planar photovoltaic cell with single-winding chains of the same quantum dots. Red- electron transporting electrode, green- hole transporting electrode.
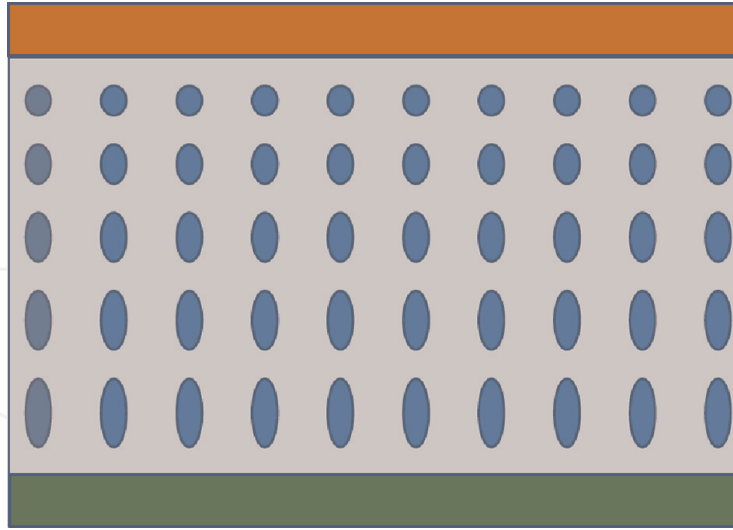
Figure 5.
Diagram of a planar photovoltaic cell with single-axis chains of quantum dots, the parameters of which (e.g. sizes) gradually change. Red- electron transporting electrode, green- hole transporting electrode.

electrons will go to the dot with a lower energy level (losing excess energy in thermalization processes), while the holes will be transported from the given dot to the dot with higher energy, which effectively leads to electron-hole separation. As before, a more general situation can be considered in which individual one-dimensional strings are different.

4. Relaxation processes for energy and spin in quantum dots important for photovoltaics applications

Possible applications of quantum dots in photovoltaics [6] call for the studies and understanding of their optical and transport properties. These properties are either controlled or strongly related to the energy and spin relaxation processes in these systems. The energy relaxation is important since it determines transport properties of the photovoltaic devices such as the probability of electron escape from the quantum dot to the glass layer and the transparent conductive oxide and, as a result, the integral photovoltaic efficiency. The spin relaxation is important since it is directly related to the coupling mechanisms responsible for the energy relaxation and allows one to find the efficient mechanisms of both the energy and the spin relaxation. In addition, the spin states are critically important for the formation of the spectra of quantum dots with several carriers (electrons and/or holes) and, thus, spin relaxation can determine the photovoltaic efficiency of the charged quantum dots in the regime of strong light irradiation, where the light intensity is sufficiently strong to produce more than one carrier per quantum dot [8].

There are different types of quantum dots applicable in photovoltaics. Let us consider ellipsoidal quantum dots serving as optical absorbers and, subsequently, source of the photo excited electrons upon their escape from the dot. The main source of the energy relaxation in single-electron quantum dots is due to various types of electron-phonon coupling, which will be analysed below. In addition, we will analyse the mechanisms of the energy relaxation in multi-electron quantum dots taking into account the electron-electron interaction. We will demonstrate that a novel mechanism of spin relaxation, different from the conventional admixing mechanism, can be relevant for

the quantum dots based on III-V group materials. Let us begin with a model of a semiconductor quantum dot applicable in photovoltaics. These dots have a variety of different properties related to their sizes and shapes. Although this variety extends the ability to use the quantum dots for nonmonochromatic light sources such as sunlight, on the other hand, it decreases the controllability of their applications. Direct system-dependent analysis of properties of quantum dots is difficult and can basically be done with the effective mass approximation as included in the Hamiltonian

$$H_0 = \frac{p^2}{2m^*} + U_e(r). \tag{9}$$

Where $\frac{p^2}{2m^*}$, is the electron kinetic energy, p is the electron momentum, m∗ is the electron effective mass, and U (r) is the effective confining potential of the quantum dot. Frequently, for model calculations the confinement is taken in the form of an anisotropic oscillator:

$$U_e(r) = 2m^* \left[\Omega_\parallel^2 (x^2 + y^2) + \Omega_z^2 z^2 \right] / 2, \tag{10}$$

where $\Omega_\parallel$ and Ω_z, are the corresponding frequencies of the anisotropic oscillator. However, this potential is well-suitable only for the description of the low-energy states of the photoexcited electrons, where wavefunction is well-localized near the potential minimum. Another form of the potential is given by $U_e(r) = 0$ for r inside the quantum dot, $U_e(r) = U$ for r outside the quantum dot, where the inside/outside boundary determines the quantum dot shape. Usual model shapes of quantum dot are ellipsoidal with an example presented in **Figure 6**. The typical scale of the quantum kinetic energy is determined by the z − axis extension of the quantum dot ω as $\hbar^2 m^* \omega^2$ with the corresponding quantity of the order of 10 meV for $\omega \sim 10$ nm and m^* of the order of 0.1 of the free electron mass. For highly excited states, with the energies above the excitation threshold of the order of 100 meV, but less than the confinement potential U, a classical description in terms of the electron trajectories becomes possible. Here emission of phonons leads to the relaxation to the lower-energy quantum states. To study the relaxation, we present electron-phonon coupling Hamiltonian (assuming the crystal volume $\equiv 1$) in the form:
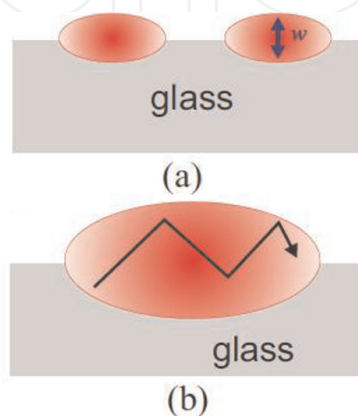
Figure 6.
(a) Two model ellipsoidal quantum dot on the surface of a glass. The vertical size of the quantum dot is denoted as w, typically of the order of 10 nm. (b) Classical trajectory of highly photoexcited electron in the quantum dot.

$$V_{e-ph} = \frac{D\sqrt{\hbar}}{\sqrt{2\zeta c}} \sum_q \sqrt{q}(de)\left(e^{-iqr}a_q^\dagger + H.c\right) \tag{11}$$

Where $a_q^\dagger$ is the creation operator for the phonon with momentum q, D is the deformation potential (D = −5.5 eV in GaAs), ζ is the crystal density, d = q/q is the phonon propagation direction, e is the phonon polarization, c is the speed of the longitudinal sound mode, and summation is taken over the momenta. We have chosen a single longitudinal phonon branch with (de) = 1, since for the transverse branches (de) = 0, taking into account only the strongest interaction with the deformational potential of the acoustic phonons.

There are different regimes of energy relaxation. The first regime is relevant for the highly-excited semiclassical states, leading to their energy loss and subsequent quantization with localization in the quantum states. The second regime is relevant for the localized states, where phonon-induced transitions occur between the low-energy quantum states in the dots. We begin with the most important for the photovoltaics semiclassical regime, where the electron states can be presented as plane waves. For the relaxation of these states shown in **Figure 6**(b) one can use the classical Boltzmann equation based on Fermi's golden rule. The energy-dependent phonon emission rate 1/τ (E) per single phonon mode with wavevector q leading to the energy relaxation is given by this rule as [9]:

$$\frac{1}{\tau(E)} = \frac{2\pi D^2 \hbar}{\hbar 2\zeta c} \int q\delta\left[E_f - E_i + \hbar\Omega(q)\right] \frac{d^3 k_f}{(2\pi)^3} \tag{12}$$

where the initial and final energy is $E_i = \frac{\hbar^2 k_i^2}{2m^*}$ and $E_f = \frac{\hbar^2 k_f^2}{2m^*}$ respectively, final electron wavevector $k_f = k_i - q$, and δ [..] − function corresponds to the energy conservation with (q) = cq. Taking into account that the characteristic wave vector k_i of a photoexcited electron is of the order of 106 cm^{-1} or higher, at the corresponding phonon momentum its energy $\hbar c k_i$ is of the order of less than one meV, that is 10 K, much less than the electron energy. As a result, the electron scattering is quasi-elastic and the occupation number of the phonons $n_B = \left[\exp\left(\frac{\hbar\Omega(q)}{T} - 1\right)\right]^{-1}$, equal to T/$\hbar\Omega$ at the room temperature T, is large. Therefore, the emission probability is greatly enhanced by the factor nB + 1. However, this occupation factor increases the phonon absorption probability as well and these processes partially compensate each other. This process leads to the energy dependence of $\frac{1}{\tau(E)}$ determined by the electron density of states, proportional to $\sqrt{E}$ and by the absolute value of the phonon momentum, also behaving as $\sqrt{E}$ and resulting in:

$$\frac{1}{\tau(E)} \approx \frac{1}{\tau_D} \frac{E}{\hbar\Omega_D} \left(\frac{m^* c^2}{\hbar\Omega_D}\right)^{1/2} \tag{13}$$

where τ_D is the nominal momentum relaxation time Ref. [9] (τ_D = 2.5 ps in GaAs), and D is the Debye phonon frequency. The time-dependence of the energy due to nearly balanced quasi-elastic emission and absorption of phonon is given by: $\frac{dE(t)}{dt} = \frac{\hbar\Omega(E)}{\tau(E)}$, where the energy goes to phonon subsystem. The numerical value of eτ is rather long, being of the order of 10^{-7} s as a result. The resulting time dependence of energy has the form:

$$E(t) = \frac{E(0)}{\left(\sqrt{\frac{E(0)}{2\sqrt{h}\tau}}t + 1\right)^2} \tag{14}$$

For the initial energy E(0) = 100 meV this estimate yields the value $\tau \sim 10$ ps, demonstrating that energy relaxation of photoexcited electrons is fast and can set up the initial condition for the diffusion through the glass layer. Taking into account that the electron velocity is of the order of 10^8 cm/s, electron during this time hits the quantum dot boundary at least 100 times. As a result, the electron can escape from the quantum dot if the escape probability per single boundary collision is higher than 10^{-2}, thus, requiring for a relatively transparent boundary between the quantum dot and the glass (see **Figure 6**(a)).

Quantum dots are often single-electron charged since they can absorb electrons from the bulk of the semiconductors. Therefore, complex states built by a photoexcited electron-hole pair inside the dot and the resident electron, usually called 'trions' Ref. [9], can be formed, as shown in **Figure 7**(a). The formation of trions extends the absorption range of quantum dots. The spectrum and the structure of a trion strongly depends on electron-electron and electron-hole coulomb interaction between electrons. The Hamiltonian of the system becomes:

$$H_0 = \frac{p_1^2}{2m^*} + \frac{p_2^2}{2m^*} + \frac{P^2}{2m_h^*} + U_e(r_1) + U_e(r_2) + U_h(R) + \frac{e^2}{\epsilon|r_1 - r_2|} + \left[\frac{e^2}{\epsilon|r_1 - R|} + \frac{e^2}{\epsilon|r_2 - R|}\right] \tag{15}$$

where r_1 and r_2 are positions of electrons (with momenta p_1 and p_2, respectively), R is the position of the hole (with mass m_h^* and the momentum P with the confinement potential Uh (R)), and ϱ is the quantum dot material dielectric constant. The process leading to the overall decrease in the escape probability is shown in **Figure 7** (b). Note that this process reduces the energy of the upper electron and increases the energy of the lower one.
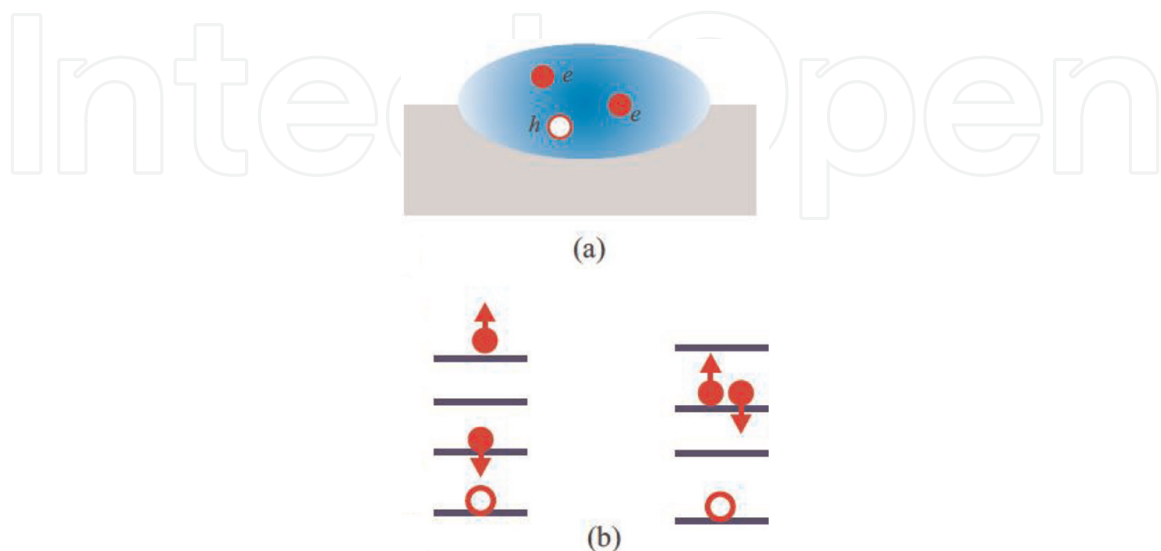

Figure 7.
(a) Trion in a photoexcited quantum dot. Electron positions are r_1 and r_2, and the hole position is R. (b) Interaction-induced transition between initial (left) and final (right) states in a quantum dot. Note that, due to the Pauli principle, this transition is possible only for the singlet electron spin state.

Despite this partial increase, the escape probability, strongly dependent on the electron energy, decreases. The corresponding energy and time scales are given by the following matrix element, where we neglected the exchange effects take only the direct interactions as: $V_C = \int \psi_f^1(r_1)\psi_f^2(r_2)\psi_f^h(R)H_C\psi_i^1(r_1)(r_2)\psi_i^h(R)d^3r_1 d^3r_2 d^3R$

where the coulomb term

$$H_C = \frac{e^2}{\epsilon|r_1 - r_2|} + \left[\frac{e^2}{\epsilon|r_1 - R|} + \frac{e^2}{\epsilon|r_2 - R|}\right] \tag{16}$$

The probability of this process is given by the time scale corresponding to the energy scale of the Hamiltonian (16), typically of the order of $\frac{e^2}{\epsilon\omega}$, that is higher than 1 meV. Therefore, these processes are very fast, being, in general, energy-conserving and dependent on the total spin of participating electrons. This energy value corresponds to short time scales of these processes, of the order of a picosecond. Then, on the top of these fast transitions, a relatively slow energy relaxation due to phonons occurs, complicated by the transitions between the localized states in the quantum dots. Yet, the energy relaxation weakly depends on these fast electron transitions since these states are localized and, therefore, the estimate of long $\tau[loc]$ given in the previous subsection is valid here as well.

Thus, understanding of energy and spin relaxation processes in quantum dots suitable for applications in photovoltaics is crucial. The energy relaxation is due to the phonon emission. It was found the relaxation times of semiclassical states of the order of 1 ps, sufficient for electron escape from the quantum dot and its contribution to the photovoltaic effects. In addition, the redistribution of electrons among the energy levels and subsequent energy evolution can be caused by the electron-electron interactions. Spin relaxation in quantum dots is caused by direct spin-phonon coupling and leads to the spin relaxation times of the order of $1-10^2$ microsecond, being the longest relaxation process in quantum dots.

Acknowledgements

Author details

Paweł Kwaśnicki[1,2]

1 Department of Physical Chemistry and Physicochemical Basis of Environmental Engineering, John Paul II Catholic University of Lublin, Institute of Environmental Engineering in Stalowa Wola, Stalowa Wola, Poland

2 Research and Development Centre for Photovoltaics, ML System S.A., Zaczernie, Poland

*Address all correspondence to: pawel.kwasnicki@mlsystem.pl

IntechOpen

References

[1] Lopez ABC, Vega AM, Lopez AL. Next Generation of Photovoltaics: New Concepts. Springer, Berlin: Eds Springer Series in Optical Sciences; 2012. ISBN 139783642233692

[2] Duan L, Hu L, Guan X, Lin C, Wu T. Quantum Dots for Photovoltaics: A Tale of Two Materials. Advanced Energy Materials. 2021;**11**(20):2100354. DOI: 10.1002/aenm.202100354

[3] Nozik AJ. Quantum dot solar cells. Physica E: Low-dimensional Systems and Nanostructures. 2002;**14**:115. DOI: 10.1016/S1386-9477(02)00374-0

[4] Tomic S. Intermediate-band solar cells: Influence of band formation on dynamical processes in InAs/GaAs quantum dot arrays. Physical Rewiev B. 2010;**82**:195321. DOI: 10.1103/PhysRevB.82.195321

[5] Kłos JW, Krawczyk M. Two-dimensional GaAs/AlGaAs superlattice structures for solar cell applications: Ultimate efficiency estimation. Journal of Applied Physics. 2009;**106**:093703. DOI: 10.1063/1.3253584

[6] Luque A, Marti A, Antolin E, Tablero C. Intermediate bands versus levels in non-radiative recombination. Physica B. 2006;**382**:320. DOI: 10.1016/j.physb.2006.03.006

[7] Nozik AJ, Beard MC, Luther JM, Law M, Ellingson RJ, Johnson JC. Semiconductor quantum dots and quantum dot arrays and applications of multiple exciton generation to third-generation photovoltaic solar cells. Chemical Reviews. 2010;**110**:6873. DOI: 10.1021/cr900289f

[8] Gantmakher VF, Levinson YB. Carrier Scattering in Metals and Semiconductors. Amsterdam: North-Holland; 1987. DOI: 10.1002/crat.2170230219

[9] Laurent S, Eble B, Krebs O, Lemaitre A, Urbaszek B, Marie X, et al. Electrical control of hole spin relaxation in charge tunable InAs/GaAs quantum dots. Physical Review Letters. 2005;**94**:147401. DOI: 10.1103/PhysRevLett.94.147401